

## Article

# Temporal Variability of Temperature, Precipitation and Drought Indices in Hyper-Arid Region of Northwest China for the Past 60 Years

Jing He <sup>1,2,3</sup>, Boshan Li <sup>1,2</sup>, Yang Yu <sup>1,2,3,4,\*</sup>, Lingxiao Sun <sup>1,2,3</sup> , Haiyan Zhang <sup>1,2,3,4</sup>, Ireneusz Malik <sup>1,4</sup>, Malgorzata Wistuba <sup>1,4</sup> and Ruide Yu <sup>1,3,4,5</sup>

- <sup>1</sup> State Key Laboratory of Desert and Oasis Ecology, Xinjiang Institute of Ecology and Geography, Chinese Academy of Sciences, Urumqi 830011, China  
<sup>2</sup> Cele National Station of Observation and Research for Desert-Grassland Ecosystems, Cele 848300, China  
<sup>3</sup> University of Chinese Academy of Sciences, Beijing 100049, China  
<sup>4</sup> Polish-Chinese Centre for Environmental Research, Institute of Earth Sciences, University of Silesia in Katowice, 60 Bedzinska, 41-200 Sosnowiec, Poland  
<sup>5</sup> School of Environment and Material Engineering, Yantai University, Yantai 264005, China  
\* Correspondence: yuyang@ms.xjb.ac.cn; Tel.: +86-18999987052

**Abstract:** The temporal variability and abrupt change analysis of temperature and precipitation in Turpan was investigated and examined based on a monthly data set of temperature, precipitation and drought indices (1960–2019) from three meteorological stations over the study area. The Yamamoto method, Mann–Kendall test, Standardized Precipitation Index (SPI), Standardized Precipitation Evaporation Index (SPEI), and Reconnaissance Drought Index (RDI) were applied to reveal temperature, precipitation and drought indices trends in their annual volumes. The conclusions were as follows: (1) in the past 60 years, the annual average temperature in the Turpan region has increased at a rate of  $0.33\text{ }^{\circ}\text{C}\cdot(10\text{a})^{-1}$ . Whereas the temperature has accelerated since the 1980s, the annual average minimum temperature has increased more than the annual average maximum temperature, and the temperature difference between winter and summer has increased since the 1990s. (2) The inter-annual, inter-decadal and normal value changes in precipitation in the Turpan region and its three meteorological stations indicated a decreasing trend during 1960–2019. Though the normal value of summer and autumn precipitation decreased and increased as a whole, the normal values of spring, summer, winter and annual precipitation in the Turpan region displayed downward trends. (3) Abrupt changes in temperature were observed in the mid-1990s, and abrupt changes in precipitation were not obvious. (4) The SPI and RDI responded quickly to precipitation and temperature, and the overall characteristics of dry and wet trend changes were consistent. When the SPEI considered the combined effect of temperature and precipitation, the SPI and SPEI are better correlated, and the SPI and RDI are better correlated than the SPEI and RDI. On the whole, the occurrence of drought has obvious regional and seasonal characteristics. These conclusions not only provide scientific data for sustainable development in Turpan but also offer scientific information to further understand the trends and periodicity of climate change and drought conditions in hyper-arid regions around the world.

**Keywords:** temperature; precipitation; drought indices; temporal variation; abrupt change analysis; Turpan



**Citation:** He, J.; Li, B.; Yu, Y.; Sun, L.; Zhang, H.; Malik, I.; Wistuba, M.; Yu, R. Temporal Variability of Temperature, Precipitation and Drought Indices in Hyper-Arid Region of Northwest China for the Past 60 Years. *Atmosphere* **2022**, *13*, 1561. <https://doi.org/10.3390/atmos13101561>

Academic Editor: Graziano Coppa

Received: 28 August 2022

Accepted: 20 September 2022

Published: 24 September 2022

**Publisher's Note:** MDPI stays neutral with regard to jurisdictional claims in published maps and institutional affiliations.



**Copyright:** © 2022 by the authors. Licensee MDPI, Basel, Switzerland. This article is an open access article distributed under the terms and conditions of the Creative Commons Attribution (CC BY) license (<https://creativecommons.org/licenses/by/4.0/>).

## 1. Introduction

Climate change is a significant global issue arousing international communities' great concern and interest and has greatly influenced water circulation and hydrological processes. Research on past and present climate variability strives to develop better and more refined approaches, which include the growing study of global and regional climate

changes and potential solutions. The IPCC (2007) [1] projects that at ocean basin, regional, and continental scales, numerous long-term climate changes will be observed, especially during the next 90 years up to 2100. In China, the government has testified that the temperature has increased by 0.4–0.5 °C from the 1800s to the 2000s, and the winter temperature has risen in a larger magnitude, especially since the 1950s (China Meteorological Administration, 2006). The climate of China is influenced by maritime and continental interactions, and its complex terrain also induces topographical influences on climate.

Under the influence of global climate change, a detailed investigation of the temporal trends of climate based on long-term temperature and precipitation series is beneficial to form a regional strategy for water resource management and provide perspectives on the connection between climate change and the hydrological cycle. Many scholars have already investigated hydrologic trends at various temporal scales in many regions of China, including precipitation. However, due to the climatic background differences, region characteristics, climate driving forces and climate responses, the response of regional climates to global climate change is asynchronous [2–5]. These studies not only analyzed historical climatic trends in different parts of China and testified to the instability and vulnerability of the climate system but also induced the complexity of regional climate and provided a context to weigh model simulations. In the previous studies of drought problems, most people have only considered the effect of precipitation on drought, such as SPI, EDI [6], GEVI, etc. Currently, the impact of rising temperature on drought has become a key factor that cannot be ignored in drought research. The most intuitive effect of air temperature on precipitation is mostly reflected in evaporation, and these indices all represent the effect of air temperature on drought by evaporation. Jian-Feng Li [7] used the standardized precipitation index (SPI) to analyze the evolution of drought characteristics in Xinjiang. The results showed that the northern Xinjiang region has a downward drought intensity trend and drought duration shortening trend. The southern Xinjiang region has a slightly increased drought intensity and drought duration trend, and the central region has a significantly increased drought intensity and drought duration trend. Xuan Junwei et al. [8] used the standardized precipitation evapotranspiration index (SPEI) to show that from 1963 to 2012, the Xinjiang region was bounded by 1987, from a general drought period to a relatively wet period. However, since the late 1990s, due to the significant increase in potential evapotranspiration, there has been a drying trend in the Xinjiang region, which indicates that the region may re-enter the drought period. Wang Naizhe [9] used the reconnaissance drought index (RDI) to analyze the five regions of the Xinjiang season scale and year scale drought characteristics. The RDI fully considered precipitation and evapotranspiration as two factors to evaluate drought, compared with only considering the precipitation drought index, it is more reasonable, the data is easy to obtain, and the calculation is simple. Xie Pei et al. concluded that the SPI is able to reflect the characteristics of drought changes in Xinjiang well, and the drought in Xinjiang has weakened in the past 55a. According to the study by Cihui et al. [10], the effect of scPDSI in drought monitoring in Xinjiang is not ideal, and the data requirements are relatively high, so it is not included in this study. Previous studies have mostly analyzed the spatio-temporal characteristics of drought in Xinjiang [7,8], and there are fewer studies on the temporal and spatial variation characteristics of drought in the study area using seasonal data. It is difficult to accurately describe the drought situation in hyper-arid areas such as Turpan. This study combines the advantages of SPI, SPEI and RDI indices, comprehensively considers the precipitation and evapotranspiration effects and compares and analyzes from multiple time scales, which is more applicable. Much of the research on the effects of climate change on drought is based on annual climate analysis, ignoring the response of drought to seasonal climate and seasonal changes in temperature and precipitation, which also have an important impact on drought. Therefore, this paper focuses on the spatio-temporal distribution characteristics, changing trends and the impact of seasonal climate change on drought in Turpan in order to deeply understand the dynamic changes in drought in Turpan under the background of climate change so as to provide a theoretical

basis for the rational use of water resources, agricultural industry structure adjustment and ecological environment prevention and control.

The Turpan basin lies in the hinterland of Eurasia, which belongs to a typical hyper-arid climate with severe scarcity of water resources. It boasts a vast area, complex natural environment and obvious regional differences in climate change [11]. Scholars have already made progress on climate change in this region, whereas research on the characteristics of climate change in small, specific areas is not comprehensive at present. The objective of this study is to investigate the climate variation in temperature, precipitation and drought conditions during the period 1960–2019 in the Turpan region. The major purposes of this study are as follows: firstly, three meteorological stations are used to analyze temperature and precipitation and their abrupt changes, which would be helpful to understand and study the local climate change. Secondly, possible reasons and impacts of temperature and precipitation in the Turpan basin are quantitatively analyzed, which will lead to a better understanding of climate variability in duration, magnitude and frequency. Thirdly, drought indices and evaluation methods are employed to study the drought conditions in the hyper-arid region.

## 2. Data and Methodology

### 2.1. Study Area

The Turpan region ( $41^{\circ}12'–43^{\circ}40'$  N,  $87^{\circ}16'–91^{\circ}55'$  E) is an olive-shaped inter-mountain basin located at the south foot of Bogda peak in the east-west branch of the Tianshan Mountains in northwest China. It is the lowest inland basin and also an important channel connecting Central Asia and northwest China. The topography of the study area is best described as a closed graben basin, higher in the northwest and lower in the southeast, which is shown in Figure 1. It boasts an area of  $6.97 \times 10^4$  km<sup>2</sup> and a length of about 300 km from east to west and 240 km from north to south. The basin in the north is a flood alluvial plain of the Tianshan river system in the north, with an altitude of 300–1500 m, relatively gentle terrain and a slope of about 2%. The southern basin is an alluvial plain formed by the Huoyanshan system. The altitude is mostly lower than sea level, and the slope is about 1%. The climate here is the typical continental arid desert climate. The annual mean temperature is only 14.6 °C, but the extreme maximum temperature is 49.6 °C, and the extreme minimum temperature is  $-29.9$  °C. Additionally, the annual precipitation is only about 16 mm, although due to the significant seasonal differences and uneven spatial and temporal distribution in this region, sometimes raindrops have evaporated before reaching the ground, which is called the “dry rain” phenomenon. Based on the analysis of temperature and precipitation changes in the study area from 1960 to 2019, this paper aims to reveal the areas climate change laws and enrich the research cases of climate change in arid areas under the background of global climate change.

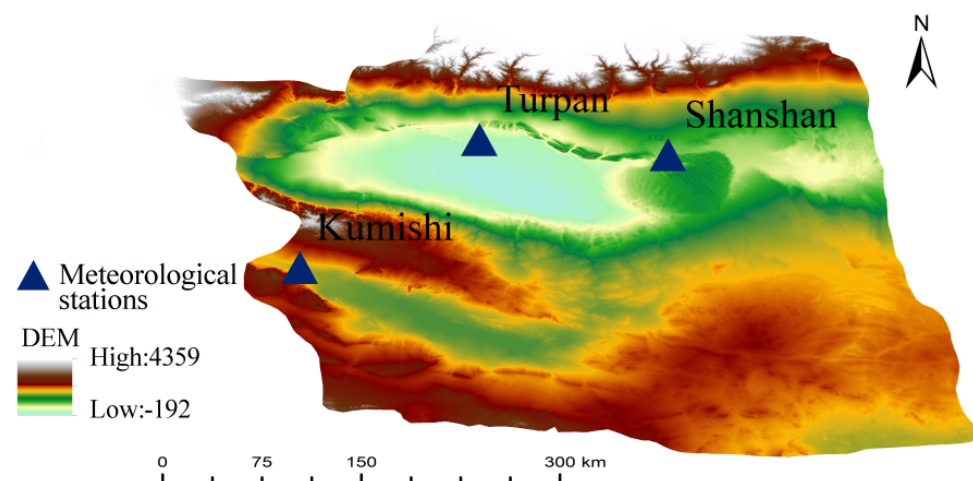


**Figure 1.** Location map showing topography of study area.

## 2.2. Data Sources and Processing

The homogeneity of temperature and precipitation data were checked very carefully in this study to increase the reliability of the data set and generate better calculations. The Turpan region governs Shanshan county, Tuokexun county and Gaochang district. Turpan, Shanshan, and Kumishi were the three meteorological stations selected as available stations inside or around the study area in order to yield a credible evaluation of the long-term trends. All the monthly temperature and precipitation data can be downloaded and checked in the China Meteorological Data Sharing Service System (<http://data.cma.cn/>, accessed on August 2022), which is a nonprofit website for research.

These three stations were established in the period 1955–1958 and thus, we selected the data from 1960 to ensure that the lengths of the data set from the different stations were clear and consistent. In this study, we divided the temperature and precipitation data into meteorological seasons, with spring defined as March to May, summer as June to August, autumn as September to November and winter as December to February (next year). All the annual and seasonal temperature and annual and decadal precipitation mean values from the Turpan region were calculated using the mean series of the three meteorological stations in the study region. Analyses and trends for periodicity and abrupt changes utilized the monthly temperature and precipitation mean values. Moreover, taking related meteorological data (e.g., wind speed, relative humidity, air temperature and air pressure) as materials as well as human activity and urban development were considered to analyze their relationships with temperature and precipitation.

## 2.3. Methods on Trend Analysis

In this study, moving average and SPEI calculation methods were used to analyze the temporal trends of temperature, precipitation and drought conditions in the Turpan region. The details about these methods are listed as follows.

### 2.3.1. Moving Average

Moving average is a popular processing method to move and filter data, which can eliminate the random fluctuation in a statistical series by taking the mean method. In addition, it takes the mean value to express changing trends of time series. As for the series of  $x$  with a sample capacity of  $n$ , the moving average series' mathematical expression is as follows:

$$\hat{x}_j = \frac{1}{k} \sum_{i=1}^k x_{i+j-1} \quad j = 1, 2, \dots, n - k + 1 \quad (1)$$

where  $k$  is the moving length. Here, we take the 5-year moving average to indicate the changing trend because 5 is odd so the average value can be added to the medium term in the time series.

### 2.3.2. Drought Indices

Three meteorological drought indices accounting for PET were considered for the analysis [12]. These indices are the Standardized Precipitation Evaporation Index (SPEI), Reconnaissance Drought Index (RDI), and Standardized Precipitation Index (SPI).

#### Reconnaissance Drought Index (RDI)

The basic form of RDI, known as the ratio of cumulative precipitation to the potential evapotranspiration during the reference period, has high sensitivity and is a widely used drought index [13]. It has three forms of expression: the initial value, a normalized RDI (RDIn), and a standardized RDI (RDIST). Using a standardized RDIST, the initial values are expressed in the form of cumulative monthly precipitation and can be calculated by month, season, or annually depending on the time scales. The calculation expression is as follows:

$$\alpha_k^{(i)} = \frac{\sum_{j=2}^k P_{ij}}{\sum_{j=1}^k PET_{ij}}, i = 1 \text{ to } N \quad (2)$$

where,  $P_{ij}$  and  $PET_{ij}$  are the precipitation and evaporation in month  $j$  of year  $i$ ,  $k$  is the time scale, and  $N$  is the total number of years of the available data time series.

### Standardized Precipitation Index (SPI)

It is difficult to directly compare precipitation for different spatial and temporal scales due to the large differences in precipitation change amplitude. The precipitation distribution is not normal, so in precipitation analysis, the distribution is assumed to be biased, and distribution probability is used to describe the change in precipitation and normalized the SPI value. The specific calculation method and physical significance are shown in the literature [14].

### SPEI Calculation

The SPEI calculation method takes into account the influence of meteorological factors on evapotranspiration. Coupled with the large evapotranspiration in the study area, this method is applicable for drought assessment in the Turpan region. The specific calculation steps are as follows:

- (1) Calculate climate level measurement—climate level measurement  $D_i$  is the difference between precipitation  $P_i$  and potential evapotranspiration  $PET_i$ :

$$D_i = P_i - PET_i \quad (3)$$

where PET was calculated using the Thornthwaite [15] method.

- (2) Establish the cumulative climate water balance series for different time scales:

$$D_n^k = \sum_{i=0}^{k-1} (P_{n-i} - PET_{n-i}), \quad n \geq k \quad (4)$$

where  $k$  is the time scale, generally in months, and  $n$  is the number of calculations.

- (3) Apply the log-logistic probability density function to fit the data series:

$$f(x) = \frac{\beta}{\alpha} \left( \frac{x - \gamma}{\alpha} \right)^{\beta-1} \left[ 1 + \left( \frac{x - \gamma}{\alpha} \right)^{\beta} \right]^{-2} \quad (5)$$

where  $\alpha$  is the scale factor,  $\beta$  is the shape factor, and  $\gamma$  is the origin parameter, which can be found by the L-moment parameter estimation method. Therefore, the cumulative probability for a given time scale is:

$$F(x) = \left[ 1 + \left( \frac{\alpha}{x - \gamma} \right)^{\beta} \right]^{-1} \quad (6)$$

The cumulative probability density was transformed to a standard normal distribution to obtain the corresponding SPEI time series of change:

$$SPEI = W - \frac{C_0 + C_1 W + C_2 W^2}{1 + d_1 W + d_2 W^2 + d_3 W^3} \quad (7)$$

where  $W$  is a parameter with the value  $\sqrt{-2 \ln(P)}$ ,  $P$  is the probability of exceeding the determined moisture gain/loss when  $p \leq 0.5$ ,  $p = 1 - F(x)$ ; and when  $p > 0.5$ ,  $p = 1 - p$ , and the sign of SPEI is reversed. The other constant terms in the formula are  $C_0 = 2.515517$ ,  $C_1 = 0.802853$ ,  $C_2 = 0.010328$ ,  $d_1 = 1.432788$ ,  $d_2 = 0.189269$ , and  $d_3 = 0.00130$ .

According to the international common drought classification standard based on drought indices, using this criterion, it is possible to determine the degree of drought change at a station in a certain month. The range  $-0.49$  to  $0.49$  is near normal,  $-0.99$  to  $-0.50$  is mild dry,  $-1.49$  to  $-1.00$  is moderately dry,  $-1.99$  to  $-1.50$  is severely dry, and less than  $-2.00$  is extremely dry. In this paper, drought indices were calculated at two different

time scales, namely, a monthly scale (RDI-1, SPI-1, SPEI-1) and an annual scale (RDI-12, SPI-12, SPEI-12).

### 2.3.3. Mann–Kendall Test

The Mann–Kendall test is an effective method for extracting the temporal variation of a series and is commonly used to monitor the analysis of hydrological and meteorological elements on time series and to test for abrupt change points. The raw data were collated and analyzed using Microsoft Excel 2016 software; the SPEI values were calculated using R programming language developed by Ross Ihaka, Robert Gentleman, from the University of Auckland, New Zealand; and the Mann–Kendall test was performed using Matlab 2018 software, Matlab is a commercial mathematics software produced by Math Works of the United States.

### 2.4. Abrupt Temporal Changes

Abrupt climate change is a kind of discontinuous phenomenon in the process of climate change, which is usually expressed by the cumulative anomaly curve of climate factors.

$$c(t) = \sum_{i=1}^t (x_i - \bar{x}) \quad (8)$$

where  $x_i$  represents the average temperature or precipitation in the  $i$ th year and  $\bar{x}$  is the average temperature or precipitation in 1960–2019. The abrupt year may be the year corresponding to the maximum absolute value index.

We chose the Yamamoto method to scrutinize the abrupt changes in temperature and precipitation series in the Turpan region. More detail is given in [16]. Given the reference year, the signal-to-noise ratio (SNR) can be expressed as follows:

$$S/N = \frac{|X_1 - X_2|}{S_1 + S_2} \quad (9)$$

where  $X_1$ ,  $X_2$ ,  $S_1$ , and  $S_2$  are the mean and standard deviation of the data series before and after the reference year, respectively. If  $SNR > 1.0$ , it is defined that there is a significant climate abrupt change at a 95% confidence interval in this year, otherwise, the abrupt change is not significant [17].

## 3. Results

### 3.1. Temporal Trends of Temperature Change

We analyzed the monthly temperature data from 1960 to 2019, including the average temperature trends, maximum and minimum temperature change and seasonal variation of temperatures in the Turpan region and its three stations with the moving average and linear regression methods.

#### 3.1.1. Trends of Inter-Annual Average Temperature

Figure 1 provides the variations in the mean annual temperature in the Turpan region from 1960 to 2019. There is a 5a moving trend of the annual temperature time series (1960–2019) for the Turpan region, which shows an increasing trend, however, some oscillations occurred from the 1960s to the 1980s but did not affect the increasing trend. The inter-annual average temperature is 11.63 °C, the minimum annual average temperature is 10.38 °C in 1960, and the maximum annual average temperature is 12.35 °C in 2016, which leaves a difference of 1.97 °C. Moreover, the present results showed that the increasing trend in temperature ( $0.33 \text{ }^\circ\text{C}\cdot(10\text{a})^{-1}$ ) was more obvious and pronounced in this area than the other regions in northwest China ( $0.27 \text{ }^\circ\text{C}\cdot(10\text{a})^{-1}$ ) [18] (Table 1).

**Table 1.** Means and anomalies in temperatures across different periods in the Turpan region from 1960 to 2019.

Period	Annual Average Temperature		Spring		Summer		Autumn		Winter	
	Mean	Anomaly	Mean	Anomaly	Mean	Anomaly	Mean	Anomaly	Mean	Anomaly
1960–1969	10.93	−0.79	14.65	−0.52	26.49	−0.48	10.10	−0.99	−7.50	−1.17
1970–1979	10.76	−0.97	14.27	−0.89	26.13	−0.84	10.29	−0.81	−7.66	−1.33
1980–1989	11.42	−0.31	14.63	−0.53	26.42	−0.55	10.73	−0.37	−6.12	0.21
1990–1999	11.77	0.048	14.84	−0.32	26.43	−0.54	11.11	0.01	−5.29	1.04
2000–2009	12.47	0.75	15.96	0.80	27.44	0.473	11.96	0.86	−5.47	0.86
2010–2019	12.99	1.27	16.63	1.46	28.89	1.93	12.41	1.31	−5.93	0.40

### 3.1.2. Annual Average Maximum and Minimum Temperature Change

Figure 2 shows the annual average maximum and minimum temperature changes in the Turpan region and its three stations from 1960 to 2019. During these 60 years, the annual maximum temperature has increased slowly (Figure 2g) with a rate of  $0.03\text{ }^{\circ}\text{C}\cdot(10\text{a})^{-1}$ . The maximum temperature was  $30\text{ }^{\circ}\text{C}$  in 2018, which is  $7\text{ }^{\circ}\text{C}$  higher than the average maximum temperature. The annual minimum temperatures have also increased (Figure 2h) with a rate of  $0.81\text{ }^{\circ}\text{C}\cdot(10\text{a})^{-1}$ . The minimum temperature was  $-6\text{ }^{\circ}\text{C}$  in 2018, which is  $6.3\text{ }^{\circ}\text{C}$  lower than the average maximum temperature. As the Kumishi station is a mountainous meteorological station, the annual average maximum temperature is quite low compared with the values in the Turpan region, and its annual average minimum temperature trend has stayed the same in these 60 years. The Shanshan station and the Turpan station are plain meteorological stations. Thus their annual average minimum temperatures are higher than the values in the Turpan region, which show a clear upward trend. In general, the annual average minimum temperature increase is greater than the annual average maximum temperature increase. The asymmetry of this linear trend is consistent with the trend of the maximum and minimum temperature in China, which also shows that the warming in this study area is more prominent in the minimum temperature. For ecological vulnerability, the extreme change in the annual average maximum and minimum temperature in recent years, especially in 2017, 2018 and 2019, provides a hint that urban expansion and Edin Lake shrinkage have already put considerable pressure on the environment of the Turpan region.

### 3.1.3. Seasonal Variation of Temperature

Figure 3 shows the monthly temperature anomaly during different periods and the temperature difference between winter and summer in the Turpan region and its three stations. The temperature change of the Turpan region from January to April is obviously larger than that of other months, indicating there is great diversity in the seasonal change of temperature between different time periods. In the 1960s and the 1970s, the temperature was relatively low in general. From November to February, the temperature was the lowest in history. In the 2010s, the average temperature in the summer was higher than the anomaly value and lower than the anomaly value in winter, indicating that the temperature difference in the winter and summer was large. The maximum temperature difference of the 60-year period appeared in 2012 ( $37\text{ }^{\circ}\text{C}$ ) (Figure 3b). Whereas in the 1990s, the temperature was significantly higher in the winter but lower in the summer. It can be observed from Figure 3b that the temperature difference between summer and winter in the 1990s was relatively small, reaching the lowest level ( $29\text{ }^{\circ}\text{C}$ ) in 1994. On the whole, since the 1980s, the temperatures in the summers have not changed much but have increased significantly in the winters. The temperature difference between winter and summer in the Turpan region began to decline in the 1980s, and the seasonality continued to weaken. All stations have their own regional characteristics in temperature anomaly and temperature difference between winters and summers. In the next section, the influence of the stations and the reasons for these characteristics are discussed.

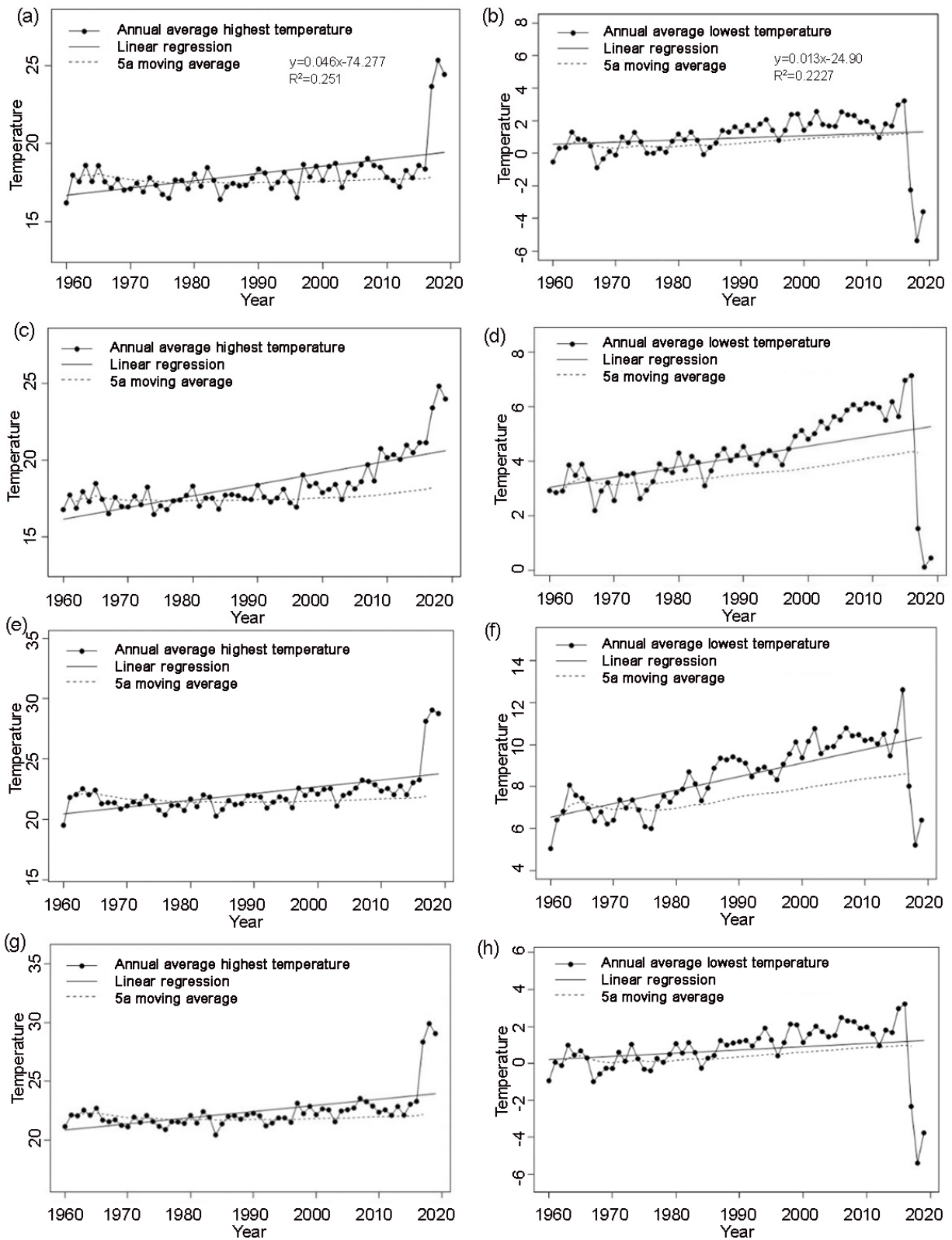


**Figure 2.** Annual average maximum (a) and minimum (b) temperature changes in the Turpan region in 1960–2019. (a,b) Kumishi (c,d) Shanshan (e,f) Turpan (g,h) Turpan region.

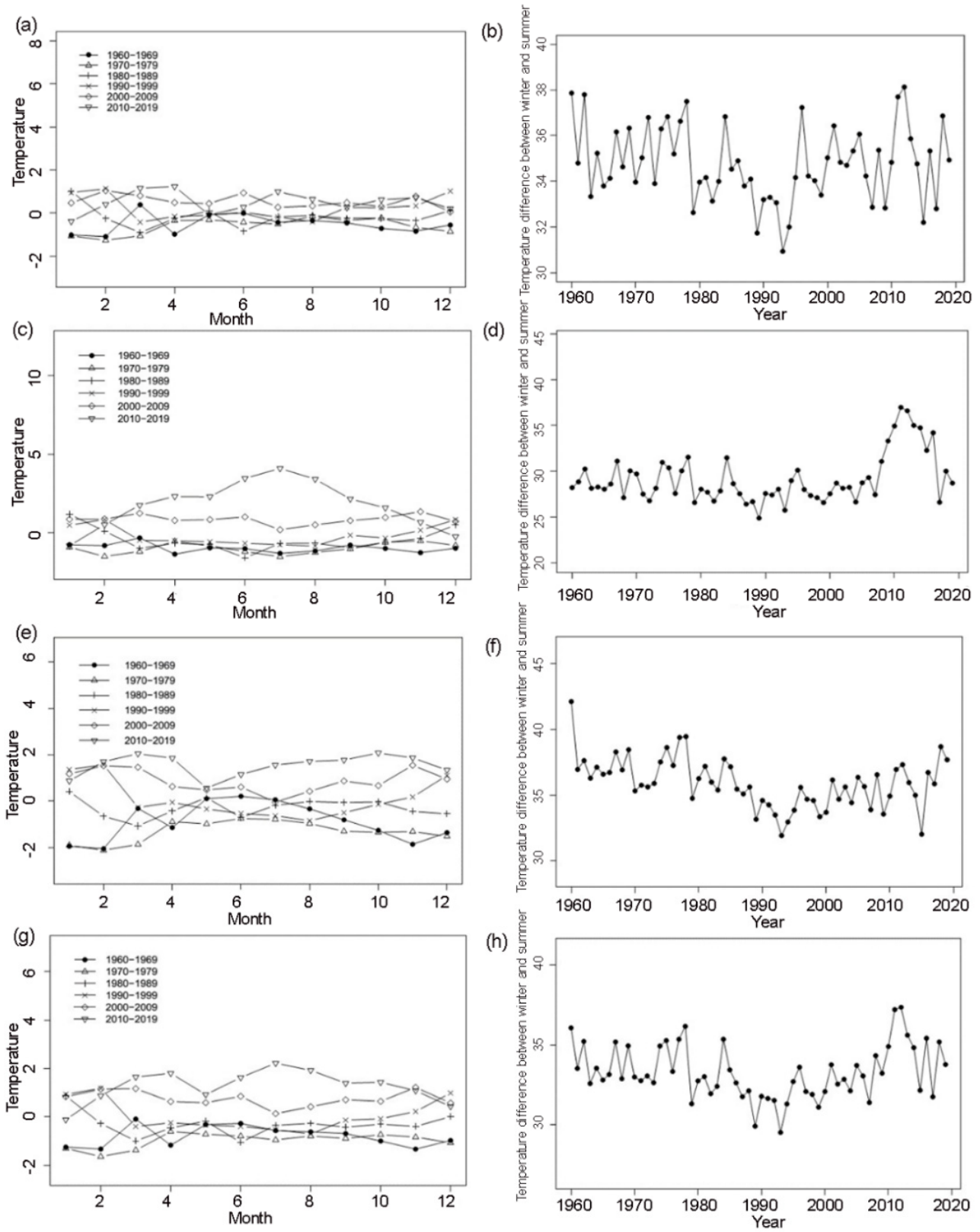


**Figure 3.** Monthly temperature anomaly during different periods (a) and temperature difference between winter and summer (b) in the Turpan region. (a,b) Kumishi (c,d) Shanshan (e,f) Turpan (g,h) Turpan region.

### 3.2. Temporal Trends of Precipitation Change

We analyzed the monthly temperature data from 1960 to 2019, including the inter-annual, inter-decadal and normal value changes in precipitation in the Turpan region and its three stations with the moving average and linear regression methods.

#### 3.2.1. Inter-Annual Precipitation Change

In Figure 4, there is a 5a moving trend of the seasonal and annual precipitation time series (1960–2019) in the Turpan region and its three stations. It is clearly observed that the annual precipitation in the Turpan region has a slightly increasing trend with little fluctuation. Additionally, the precipitation was relatively low around the 1980s and from 2009 to 2017 (Figure 4t) and comparatively high from 1992 to 1996 and from 2001 to 2003. Similar to the Turpan region, the annual precipitation at the three stations all reported small fluctuations. In more detail, the annual precipitation at the Kumishi station underwent an increase (1962–1966), a stable period (1967–1986), and an increase (1987–2018) (Figure 4q). At the Shanshan station, the precipitation experienced a wave trough in 1969 and a wave crest in 2005 during the oscillation process (Figure 4r). The Turpan station had the opposite precipitation trend in this period and failed to change the whole precipitation trend. The annual precipitation experienced major fluctuations in the 1960s, which is shown by the wave crest in 1964 (Figure 4s).

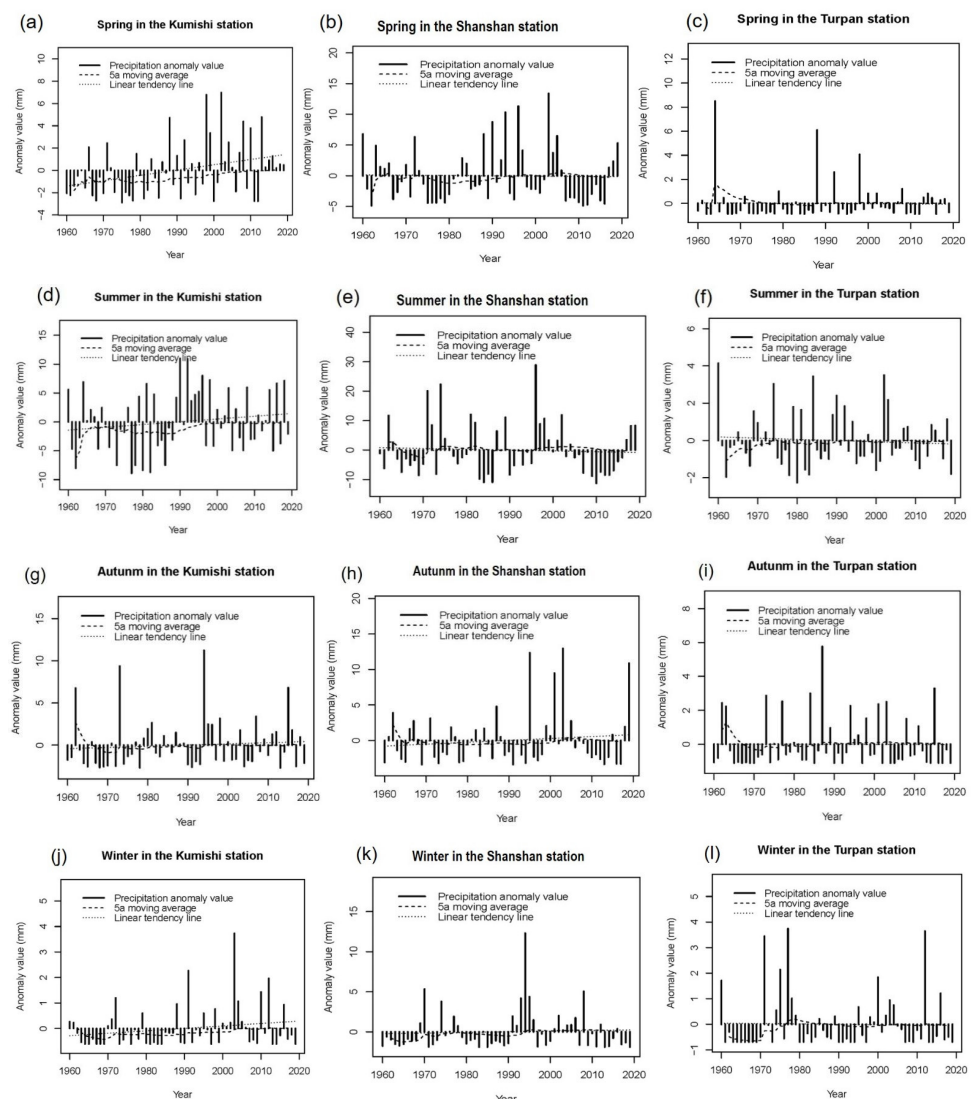
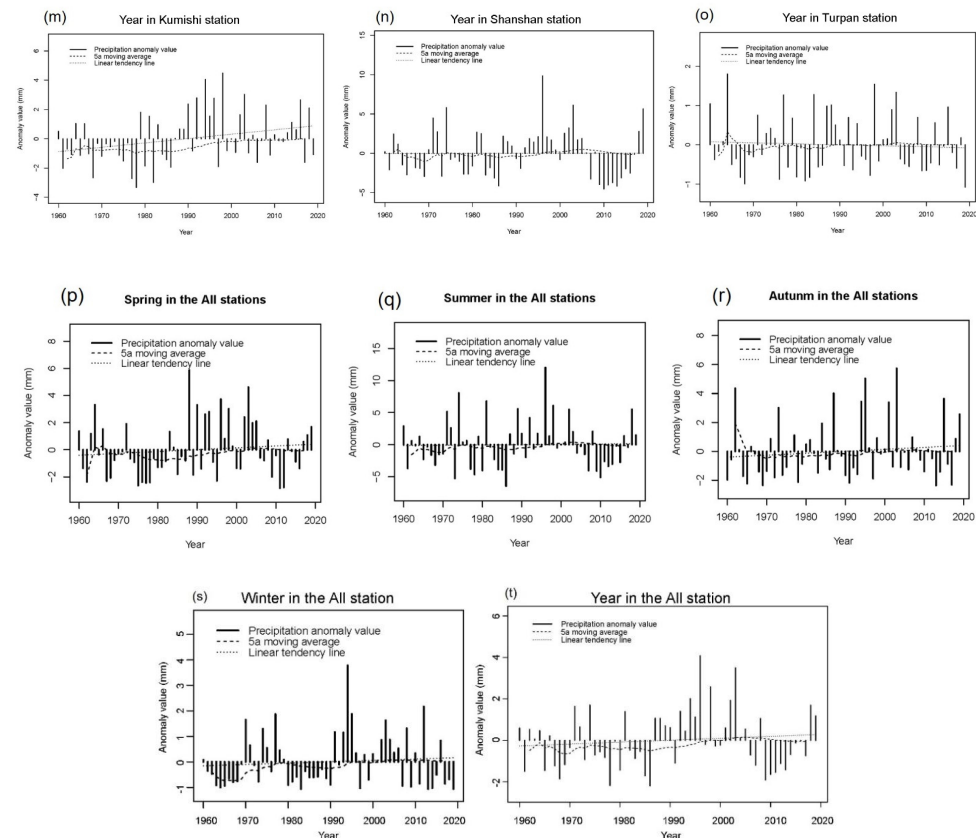


Figure 4. Cont.



**Figure 4.** Anomaly value, 5a moving average and linear tendency of the precipitation in the Turpan region.

Although the seasonal precipitation indicates diversity, the annual precipitation in the Turpan region underwent an increasing trend (Figure 2). At first, the spring precipitation in the Turpan region had an overt upward trend and displayed an oscillating process: increasing (1960–1966), decreasing (1967–1980), increasing (1981–2005) and decreasing (2006–2019) (Figure 2d). Then, the summer precipitation was stable overall, which manifested the oscillating process: increasing (1960–1975), decreasing (1976–1990) and stable (1991–2019) (Figure 2h). Then, the autumn precipitation had an upward trend and then stabilized (Figure 4l). In the end, the winter precipitation presented a small fluctuating process: decreasing (1960–1969), increasing (1970–1979), decreasing (1980–1990), increasing (1991–2010) and decreasing (2011–2019) (Figure 4p). Whereas the seasonal precipitation for the three stations reported small changes, with the fluctuations being inconsistent with regional differences. The reasons for these fluctuations will be discussed in the next section.

The spring precipitation in the Turpan station had a downward trend at a significance level of 0.001 (Table 2), which decreased at a rate of  $-0.002 \text{ mm} \cdot (10a)^{-1}$ . The positive trend of summer precipitation at the Kumishi station was detected at a significance level of 0.1 (Table 2), which increased at a rate of  $0.048 \text{ mm} \cdot (10a)^{-1}$ . An upward trend of annual precipitation was discovered for the Turpan region, though spring and summer precipitation at the Turpan station and Shanshan station showed a downward trend. The increasing rate for the Turpan region was  $0.009 \text{ mm} \cdot (10a)^{-1}$ , while the rates for the Kumishi, Turpan and Shanshan stations were 0.03,  $-0.003$  and  $0.001 \text{ mm} \cdot (10a)^{-1}$ , respectively. This indicates that the increased rate of annual precipitation at the Kumishi station was the greatest among the three stations, followed by the Shanshan station. The seasonal changing trends for the three stations are shown in Table 2. The increasing rate of precipitation at the Kumishi station was the maximum in the spring and summer, then followed by autumn and winter, which was the minimum. The changes in the rate of precipitation at the Turpan station were very small, and the autumn precipitation remained the same. However, the spring, summer and winter precipitation indicated a downward trend.

Moreover, the change in the rate of summer precipitation at the Shanshan station was the minimum, followed by spring precipitation, while the autumn precipitation showed an increasing trend.

**Table 2.** Tendency rates of seasonal and annual precipitation changes in the Turpan region.

Region	Spring (mm·(10a) <sup>-1</sup> )	Summer (mm·(10a) <sup>-1</sup> )	Autumn (mm·(10a) <sup>-1</sup> )	Winter (mm·(10a) <sup>-1</sup> )	Year (mm·(10a) <sup>-1</sup> )
Kumishi	0.048	0.048	0.014	0.01	0.03
Turpan	−0.002	−0.006	0	−0.001	−0.003
Shanshan	−0.005	−0.027	0.027	0.008	0.001
Turpan region	0.014	0.005	0.013	0.005	0.009

### 3.2.2. Inter-Decadal Precipitation Change

Figure 5 shows the inter-decadal change of precipitation in the Turpan region and its three meteorological stations. The annual precipitation in the Turpan region was comparatively higher in the 1970s, 1980s and 2000s, while it was low in the 1960s, 1980s and 2010s. Especially after 2001, it was 3.8 mm higher than the long-term average annual value. For seasonal precipitation, the spring (March to May) average precipitation in the 1970s was extremely low, however, it increased gradually in the 1980s and 1990s, while the precipitation after 2001 the precipitation remained a bit lower than the long-term average annual value. The summer (June to August) average precipitation was relatively low in the 1960s and 2010s but increased soon after the 1970s, which remained an increasing trend for 40 years. Except in the 1970s, the autumn precipitation in the other periods remained lower than the long-term average annual value, even in the 2000s when the value was 5.3 mm lower than the long-term average annual value. The winter precipitation in all periods was lower than the long-term average annual value, especially in the 1990s.

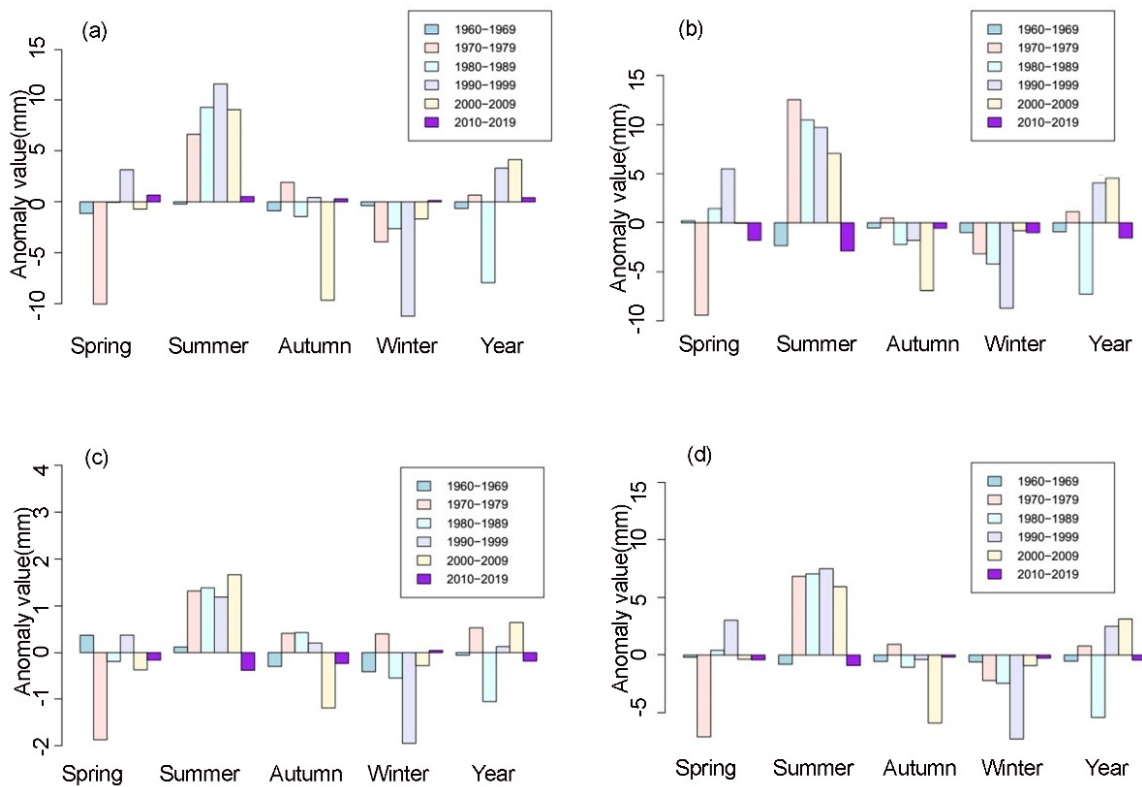


**Figure 5.** Seasonal and annual precipitation anomaly for different time scales in the Turpan region. (a) Kumishi (b) Shanshan (c) Turpan (d) Turpan region.

There are regional diversities in the inter-decadal change of seasonal and annual precipitation for the Turpan region (Figure 5). Taking the Kumishi station as an example, in the 2010s, the annual precipitations were higher than the long-term average annual value by 0.5 mm. The spring precipitation in the 1980s and 2010s showed the opposite trend to the annual precipitation value. The summer precipitation was higher than the long-term average annual value in the 1980s and 1990s, and the autumn precipitation was also higher than the long-term average annual value in the 1990s and 2010s. The winter average precipitation was similar to the long-term average annual value except for the 2010s. The inter-decadal changes in seasonal and annual precipitation in the Shanshan station were similar to those in the Turpan region (Figure 5b,c), although several regional differences can be observed. The spring precipitation was lower in the 2010s, and the summer precipitation was lower in the 1960s and 2010s. Both the autumn precipitation and the winter precipitation were lower in the 1980s and 2010s. In addition, the Turpan station was quite different from those in the Turpan region (Figure 5b,c). Both the spring precipitation and the summer precipitation showed the opposite trend compared to the annual precipitation in the 1960s. The autumn precipitation showed the opposite trend in the 1980s, and the winter precipitation showed the opposite trend in the 1970s and 2010s.

### 3.2.3. Normal Value Precipitation Change

The WMO adopted the climate normal to utilize for climatologic analysis and confrontation in the conventional 30-year period [19]. In this study, four 30-year periods (1960–1989, 1970–1999, 1980–2009 and 1990–2019) were calculated. The climate normal values of seasonal and annual precipitation in the Turpan region and its three stations are shown in Table 3. From 1960–1989 to 1970–1999, the climate normal of the seasonal and annual precipitation in the Turpan region changed by  $-0.460$ ,  $-1.061$ ,  $-0.222$ ,  $-0.392$  and  $-0.534$  mm, respectively. The variations from 1970–1999 to 1980–2009 were  $-0.541$ ,  $0.137$ ,  $-0.341$ ,  $0.043$  and  $-0.176$  mm, respectively, and the variations from 1980–2009 to 1990–2019 were  $0.108$ ,  $0.027$ ,  $0.174$ ,  $-0.124$  and  $0.046$  mm, respectively. These results indicate that although the normal value for spring, summer, autumn, winter and the annual precipitation decreased or increased, the annual precipitation normal value increased in general.

**Table 3.** Changes in precipitation normal value in the Turpan region.

Region	Period	Spring (mm)	Summer (mm)	Autumn (mm)	Winter (mm)	Year (mm)
Kumishi	(1960–1989)–(1970–1999)	−0.654	−1.467	−0.508	−0.156	−0.696
	(1970–1999)–(1980–2009)	−0.649	−0.886	0.087	−0.132	−0.395
	(1980–2009)–(1990–2019)	−0.319	−0.856	0.040	−0.147	−0.320
Turpan	(1960–1989)–(1970–1999)	0.057	−0.003	−0.089	−0.023	−0.015
	(1970–1999)–(1980–2009)	−0.147	−0.038	−0.002	0.272	0.021
	(1980–2009)–(1990–2019)	0.069	0.053	0.266	−0.138	0.063
Shanshan	(1960–1989)–(1970–1999)	−0.783	−1.712	−0.069	−0.997	−0.890
	(1970–1999)–(1980–2009)	−0.828	1.334	−1.108	−0.011	−0.153
	(1980–2009)–(1990–2019)	0.574	0.884	0.216	−0.087	0.397
Turpan region	(1960–1989)–(1970–1999)	−0.460	−1.061	−0.222	−0.392	−0.534
	(1970–1999)–(1980–2009)	−0.541	0.137	−0.341	0.043	−0.176
	(1980–2009)–(1990–2019)	0.108	0.027	0.174	−0.124	0.046

Though the precipitation normal values for the three stations were almost consistent with those of the Turpan region as a whole, they also diversified in different areas (Table 3). From 1960–1989 to 1970–1999, the normal values of annual and seasonal precipitation at the Kumishi station changed by  $-0.654$ ,  $-1.467$ ,  $-0.508$ ,  $-0.156$  and  $-0.696$  mm, respectively, the variations of normal values were  $-0.649$ ,  $-0.886$ ,  $0.087$ ,  $-0.132$  and  $-0.395$  mm from 1970–1999 to 1980–2009, and the variations from 1980–2009 to 1990–2019 were  $-0.319$ ,  $-0.856$ ,  $0.040$ ,  $-0.147$  and  $-0.320$  mm, respectively. Thus, except for the autumn, the normal values of annual and other seasonal precipitation had a downward change, and the annual precipitation normal values decreased in general. From 1960–1989 to 1970–1999, the normal values of seasonal and annual precipitation at the Turpan station changed by  $0.057$ ,  $-0.003$ ,  $-0.089$ ,  $-0.023$  and  $-0.015$  mm, respectively, the variations of normal values

were  $-0.147$ ,  $-0.038$ ,  $-0.002$ ,  $0.272$  and  $0.021$  mm from 1970–1999 to 1980–2009, and the variations from 1980–2009 to 1990–2019 were  $0.069$ ,  $0.053$ ,  $0.266$ ,  $-0.138$  and  $0.063$  mm, respectively. Similar to those in the Turpan station, the variations for the normal values of seasonal and annual precipitation at the Shanshan station were  $-0.783$ ,  $-1.712$ ,  $-0.069$ ,  $-0.997$  and  $-0.890$  mm, respectively, from 1960–1989 to 1970–1999,  $-0.828$ ,  $1.334$ ,  $-1.108$ ,  $-0.011$  and  $-0.153$  mm from 1970–1999 to 1980–2009, and the variations from 1980–2009 to 1990–2019 were  $0.574$ ,  $0.884$ ,  $0.216$ ,  $-0.087$  and  $0.397$  mm, respectively. All of these show that the normal value of summer and autumn precipitation that increased and decreased as a whole, and the normal values of spring, winter and annual precipitation displayed downward trends in the four 30-year periods.

### 3.3. Abrupt Change Analysis

The results of Yamamoto method on the abrupt change in the annual temperature and precipitation time series (1960–2019) in the Turpan region are shown in Figure 6. The temporal trends were investigated by the Yamamoto method, and it was observed that temperature presented statistically significant increasing trends while precipitation presented statistically significant decreasing trends. The largest absolute value of annual average temperature anomaly curve in the Turpan region was in 1996, from then on temperature became higher from the lowest point and continues to grow until now. Using the Yamamoto method to testify whether this anomaly qualified as an abrupt climate change, the result showed that the ratio of 1996 is 1.343, which was  $>1.0$ . Thus, we conclude that 1996 can be qualified as an abrupt year, and the average temperature of 1996–2019 is  $16.43$  °C, which is  $1.53$  °C higher than that before the abrupt year.

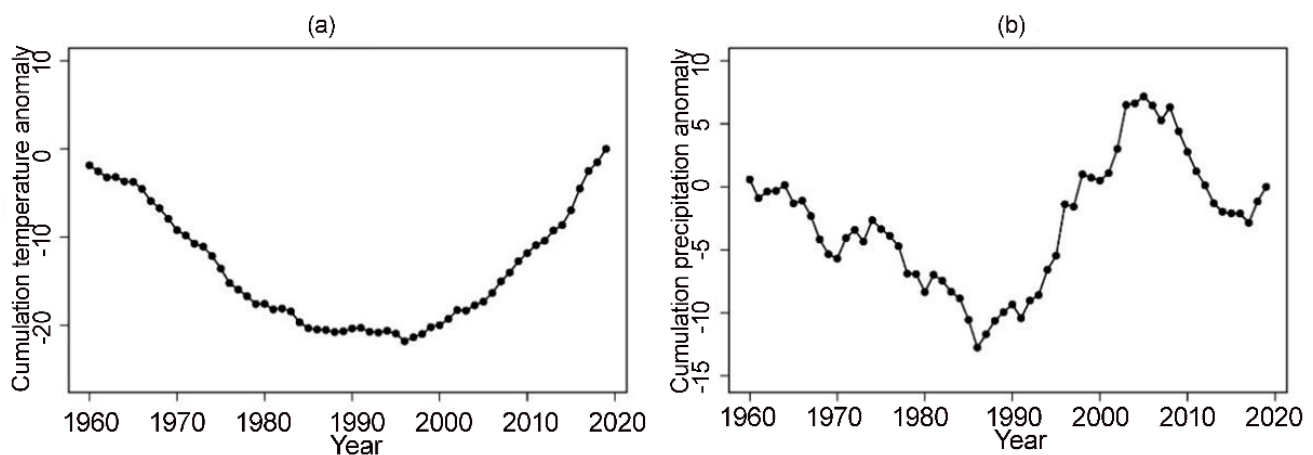


**Figure 6.** Annual average temperature (a) and precipitation (b) cumulation anomaly curves in the Turpan region from 1960 to 2019.

Figure 6b shows the annual average precipitation cumulation anomaly curves in the Turpan region. From the 1960s to the mid-1980s, precipitation declined sharply, then rose rapidly till 2005. The year with the largest absolute value was 1986, and it was the turning point for an increasing precipitation trend. After 1986, the precipitation continued to grow, reaching the highest value in 2005. We also used the Yamamoto method to testify whether this anomaly qualified as an abrupt climate change, the result showed that the ratios of 1986 and 2005 were 0.315 and 0.259, respectively, which are both  $<1.0$ , so the abrupt change of precipitation in 1986 and 2005 is not considered significant.

### 3.4. Drought Indices Trends on Different Time Scales

According to Figure 7, the Turpan region drought indices of different time scales have different sensitivity with time. The shorter the time scale, the more frequent the dry and wet fluctuations; otherwise, the longer the time scale, the flatter the dry and wet fluctuations. On the monthly scale, SPEI, SPI and RDI fluctuated greatly from 1960 to 2019,

indicating that the alternation of dry and wet was more frequently influenced by monthly scale precipitation and temperature (Figure 7a–c). During the study period, near normal, mild dry, moderately dry and severely dry changed similarly in all drought events, while SPI-1 and RDI-1 indexes increased, and drought decreased. However, the SPEI-1 index decreased, and the drought increased. On the annual scale, according to Figure 7d–f, the SPEI index changed significantly in the Turpan region, and drought increased; the SPI index increased significantly in the Turpan region, and drought decreased; while the RDI index changed more gently in the Turpan region, and drought decreased. The month and year scale changes in Turpan indicate that the month scale fluctuates strongly, indicating that the month scale drought indices are more sensitive to changes in precipitation and temperature over the shorter time scale than the year scale, and more accurately reflect short-term drought events. The annual scale drought indices are more sensitive to meteorological factors than the month scale, and the response to short-term drought is inaccurate due to the relatively long time scale and drought, which is a clear indicator of the duration and developmental trend of drought. Therefore, the reasonable application of drought indices at different scales can be helpful for early warning and prediction of drought in the Turpan region.

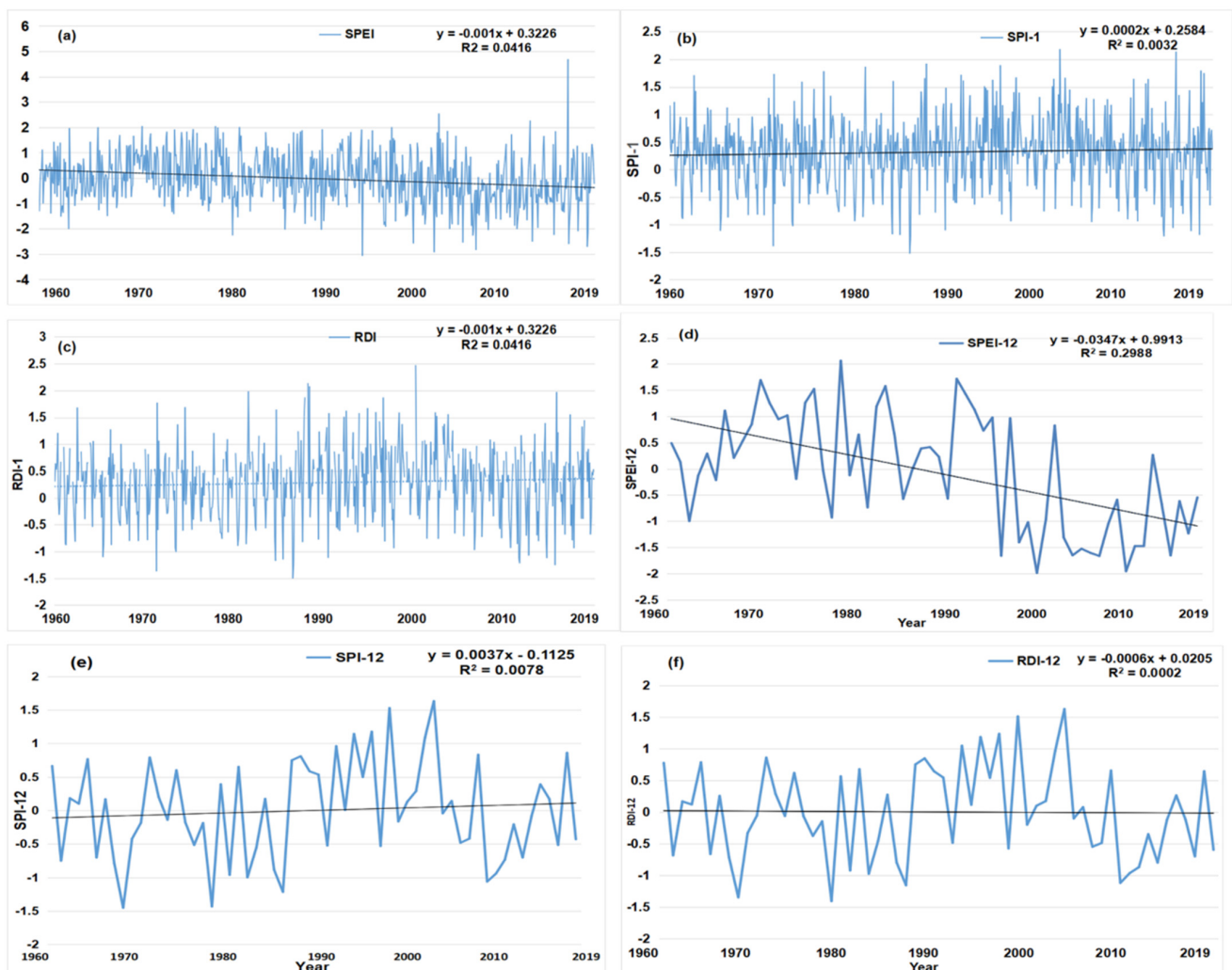


Figure 7. Turpan region drought indices time scale drought variation. (a–c) Monthly scale. (d–f) Annual scale.

### 3.5. Drought Frequency Analysis

The annual-scale SPI showed variation from 1960 to 2019 between  $-1.45$  and  $1.63$ , and for the drought events near normal, mild dry and moderately dry represented  $40.00\%$ ,  $30.00\%$ , and  $6.67\%$ . The annual scale SPEI showed variation from 1960 to 2019 between  $-1.98$  and  $2.06$ , and for the drought events near normal, mild dry, moderately dry, and severely dry accounted for  $21.67\%$ ,  $15.00\%$ ,  $11.67\%$ , and  $13.33\%$ . Extreme drought events mostly occurred in the summer and winter months. The year-scale RDI shows a variation between  $-1.4$  and  $1.62$  from 1960–2019, with for the drought events near normal, mild dry and moderately dry accounted for  $40.00\%$ ,  $21.67\%$  and  $6.67\%$ , respectively. The Turpan region SPEI, SPI and RDI indexes mostly decreased with the increase of drought grade and SPEI frequency for severely dry grade. SPI and RDI have similar results, SPEI occurs in near normal and mild dry and is lower than the other two drought indexes, and in moderately dry and severely dry is higher than the other two drought indexes (Figure 8).

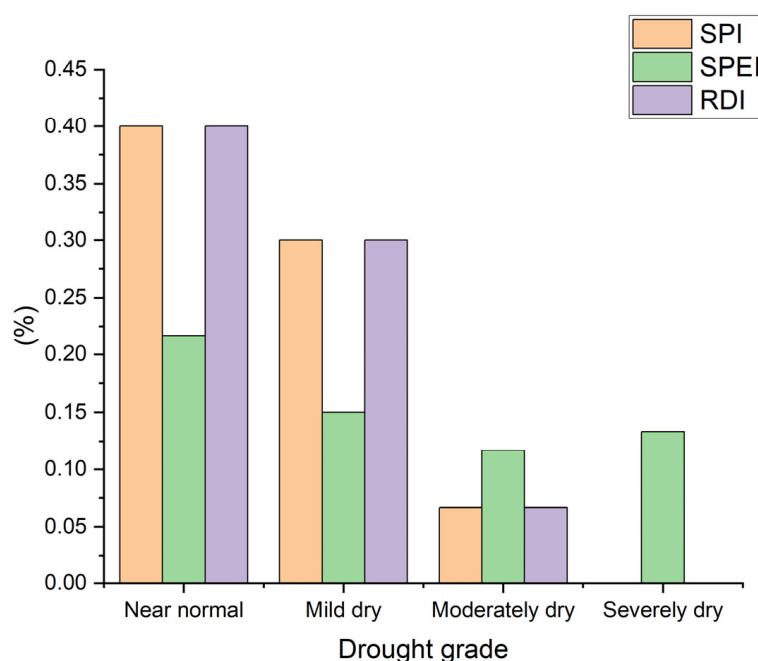
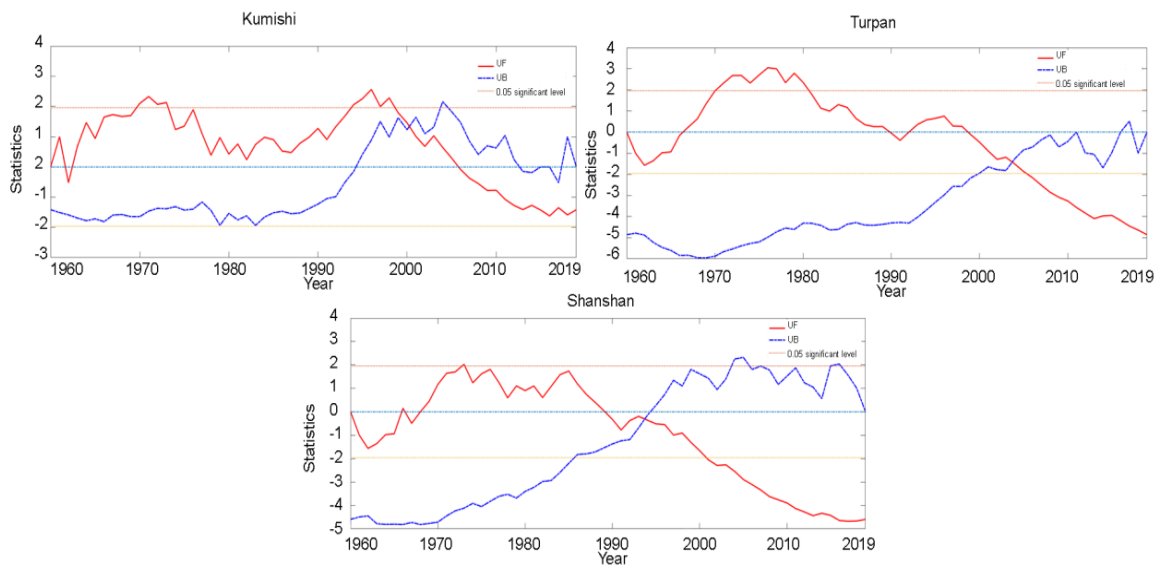


Figure 8. Drought grade for Turpan region annual scale from 1960–2019.

### 3.6. Characteristics of the Evolution of Inter-Annual Drought Trends in SPEI

The z-values of the SPEI index for all three meteorological stations in the Turpan region from 1960 to 2019 were less than 0, indicating an increasing trend of drought in the region. In terms of the individual stations, Shanshan and Kumishi both had z-values less than  $-2.58$  on an annual scale, passing the 99.9% significance test, meaning that these two stations show a highly significant increasing trend in drought. The Turpan site has a z-value of  $-1.40952$  on an annual time scale, which is not significant.

As shown in Figure 9, the annual scale SPEI indices for Turpan and Shanshan show a highly significant decreasing trend with a tendency of  $-0.048/10a$  and  $-0.041/10a$ , respectively, in the last 60 years ( $p < 0.001$ ). This indicates that these two sites show a highly significant aridity trend. In Kumishi, the SPEI values were 2.15 and  $-2.22$  for the wettest and driest years of the period 1961–2019, respectively, and the M–K trend was  $-0.014/10a$ . The results of the M–K trend test indicate that the year 2000 was the beginning of the aridification mutation in Kumishi. In Turpan, the SPEI values were 2.31 and  $-2.31$  for the wettest and driest years of 1979 and 2011, respectively, and the M–K trend test showed the onset of the aridity mutation in Turpan in 2003–2004. In Shanshan, the two wettest and driest years were 1984 and 2005, with SPEI values of 2.13 and  $-2.16$ , respectively, and the M–K trend test showed the onset of the aridity mutation in Shanshan in 1993–1994.



**Figure 9.** M–K mutation test curves for Turpan region annual scale SPEI indices 1960–2019.

3.7. Correlation Analysis between Turpan Region SPEI and Meteorological Elements

Using the Spearman correlation analysis method for the SPEI, SPI, RDI, minimum temperature, maximum temperature, mean temperature, precipitation and potential evapotranspiration, analysis found that (Figure 10): at the annual scale SPEI and PRE ( $R = 0.27, p < 0.01$ ), TMX ( $R = 0.76, p < 0.05$ ) showed a positive correlation; PET was negatively associated with SPEI ( $R = -0.06, p < 0.05$ ); PET ( $R = -0.4, p < 0.01$ ), TMX ( $R = -0.31, p < 0.01$ ), TMP ( $R = -0.38, p < 0.01$ ) were all negatively correlated with SPI; PRE was positively correlated with SPI ( $R = 0.3, p < 0.01$ ); PET ( $R = -0.11, p < 0.01$ ), TMX ( $R = -0.31, p < 0.01$ ), TMP ( $R = -0.087, p < 0.01$ ), and PRE ( $R = -0.042, p < 0.05$ ) were all negatively correlated with RDI. The results show that the drought index was the most sensitive to precipitation. All of these showed a positive correlation. Precipitation and maximum temperature are the main factors influencing the drought change. The potential evapotranspiration, minimum temperature, maximum temperature and mean temperature were all negatively associated with the drought index. The correlation coefficient between the drought index and the mean temperature was small, which shows that its effect on drought change is small (Figure 10).

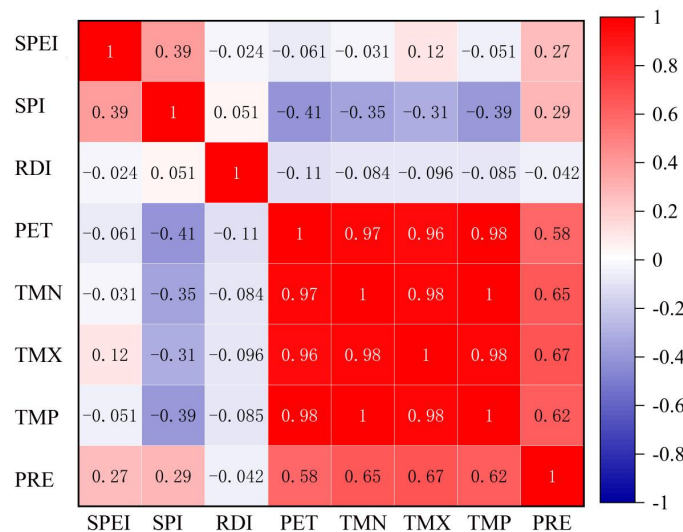


**Figure 10.** Correlation between different meteorological factors and drought index (PET: Potential Evapotranspiration; TMN: Minimum temperature; TMX: Maximum temperature; TMP: Mean temperature; PRE: Precipitation).

## 4. Discussion

### 4.1. Possible Reasons for Temperature and Precipitation Changes

The Turpan region's special geographical location and terrain make it more sensitive to temperature change. Its urban forest coverage area is less than 2%, though mainly located in the oasis due to excessive dependence on traditional farming technology and utilization of underground water resources, the agriculture land deterioration is a serious issue to address. Thus, the Turpan region is regarded as a sensitive climate response area. The increasing trend in temperature ( $0.33\text{ }^{\circ}\text{C}\cdot(10\text{a})^{-1}$ ) is much higher than global average. As in Turpan region, the population has already increased from 0.4 million to above 0.6 million in the past 20 years. With the acceleration of urbanization, the density of urban population increases and the rate has reached 37%, leaving mainly population inhabiting the county towns. The construction area of Turpan city has increased dramatically with the fixed assets investment reaching 20 times what it was in the 1990s in 2016.

### 4.2. Disadvantages of the Climatic Drought Indices

According to the above analysis of the change trend, correlation and drought frequency of the three drought indexes (SPI, SPEI and RDI). First of all, the change trend of the three drought indexes is not consistent. Some studies show that the overall climate is warmer and wet, and the vegetation is constantly improving, which reflects the decreasing trend of drought in Xinjiang. In this study, the SPI index trend change was the same as the overall climate change in Xinjiang, while the SPEI index was significantly different. The study of Guo Dong et al. showed that the change trend reflected by the SPEI index in eastern Xinjiang and the eastern region of southern Xinjiang is contrary to the change in Xinjiang as a whole. It is possible that the SPEI caused the calculation of the PET and the actual situation. Essentially, the SPI, RDI, and SPEI are defined and calculated based on similar methods, and their values have the same statistical significance. The SPI considers only the climate water supply, while the RDI and the SPEI are formulated by considering both the climate water supply and the demand aspects. From this point of view, the RDI and SPEI outperform the SPI. In relatively arid areas, ET is controlled by precipitation and water availability, so that SPI and RDI will perform better than SPEI. Xu et al. [20] studied the drought changes in China over the past half-century based on SPI3, RDI3 and SPEI3, where SPI and RDI are more suitable than SPEI. In addition, both RDI and SPEI are sensitive to PET. Therefore, PET is very important for drought assessment based on the RDI and SPEI indices (see Figure 8). We showed that the PET-based index varies somewhat in significance and magnitude between the exponents. The differences in drought prediction due to different indices highlight the importance of the careful consideration of the drought index in future evaluations.

## 5. Conclusions

This paper presents an updated revision of climate change and drought studies in the Turpan region from 1960 to 2019, demonstrating regional climatic variability and drought conditions in the hyper-arid Turpan region of China. It can be seen that consistent with global trends, there are several differences and seasonal and inter-annual variability in the Turpan region temperature and precipitation records. The results show that the temperature of the Turpan region has increased, and the temperature difference between summers and winters has become more vivid than before. This phenomenon may have an impact on the water cycle in small areas, and an increased risk of drought. The annual precipitation presented an increasing trend in this region during 1960–2019, while the increasing rate can be ignored to some extent. The Turpan region showed a significant overall trend towards drought ( $p < 0.001$ ). Temporally, SPEI values from 1960–2019 showed a significant cyclical pattern across time scales, with the frequency of drought events decreasing and the drought cycle lengthening as the SPEI time scale increased. This study provides a scientific basis for the changing characteristics of climate and drought in hyper-arid regions.

**Author Contributions:** Conceptualization, J.H.; writing—original draft preparation, J.H. and B.L.; writing—review and editing, R.Y., L.S., H.Z., I.M. and M.W.; supervision, Y.Y. and R.Y.; funding acquisition, Y.Y. All authors have read and agreed to the published version of the manuscript.

**Funding:** This research was funded by the CAS Pioneer Hundred Talents Program (E2250109); National Natural Science Foundation of China (No. 42107084); and the “High-level Talents Project” (Y871171) of Xinjiang Institute of Ecology and Geography, Chinese Academy of Sciences.

**Institutional Review Board Statement:** Not applicable.

**Informed Consent Statement:** Not applicable.

**Data Availability Statement:** Data set available on request to corresponding authors.

**Conflicts of Interest:** The authors declare no conflict of interest.

## References

1. Solomon, S.; Qin, D.; Manning, M.; Chen, Z.; Marquis, M. Summary for Policymakers. In *Climate Change 2007: The Physical Science Basis*; Contribution of Working Group I to the Fourth Assessment Report of the Intergovernmental Panel on Climate Change (IPCC); Cambridge University Press: Cambridge, UK, 2007.
2. Bo, L.I.U.; Jinming, F.; Zhuguo, M.A.; Rongqing, W.E.I. Characteristics of Climate Changes in Xinjiang from 1960 to 2005. *Clim. Environ. Res.* **2009**, *14*, 414–426.
3. Ren, G.Y.; Xu, M.Z.; Chu, Z.Y.; Guo, J.; Li, Q.X.; Liu, X.N.; Wang, Y. Changes of Surface Air Temperature in China During 1951–2004. *Clim. Environ. Res.* **2005**, *10*, 717–727.
4. Yang, L.; Villarini, G.; Smith, J.A.; Tian, F.Q.; Hu, H.P. Changes in seasonal maximum daily precipitation in China over the period 1961–2006. *Int. J. Climatol.* **2013**, *33*, 1646–1657. [[CrossRef](#)]
5. Zhang, A.J.; Zheng, C.M.; Wang, S.; Yao, Y.Y. Analysis of streamflow variations in the Heihe River Basin, northwest China: Trends, abrupt changes, driving factors and ecological influences. *J. Hydrol.-Reg. Stud.* **2015**, *3*, 106–124. [[CrossRef](#)]
6. Morid, S.; Smakhtin, V.; Moghaddasi, M. Comparison of seven meteorological indices for drought monitoring in Iran. *Int. J. Climatol.* **2006**, *26*, 971–985. [[CrossRef](#)]
7. Li, J.; Zhang, Q.; Chen, X.; Bai, Y. SPI-based Drought Variations in Xinjiang, China. *J. Appl. Meteorological Sci.* **2012**, *23*, 322–330.
8. Xuan, J.; Zheng, J.; Liu, Z. SPEI-based Spatiotemporal Variation of Drought in Xinjiang. *Arid Zone Res.* **2016**, *33*, 338–344.
9. Wang, N.; Jing, Y.; Xu, X.; Hanggoro, W. Application of RDI index in drought monitoring of five regions in Xinjiang. *Arid Land Geogr.* **2020**, *43*, 99–107.
10. Ci, H.; Zhang, Q.; Xiao, M. Evaluation and comparability of four meteorological drought indices during drought monitoring in Xinjiang. *Acta Sci. Nat. Univ. Sunyatseni* **2016**, *55*, 124–133.
11. Chen, Y.; Xu, C.; Hao, X.; Li, W.; Chen, Y.; Zhu, C.; Ye, Z. Fifty-year climate change and its effect on annual runoff in the Tarim River Basin, China. *Quat. Int.* **2009**, *208*, 53–61.
12. Wang, W.G.; Xing, W.Q.; Shao, Q.X. How large are uncertainties in future projection of reference evapotranspiration through different approaches? *J. Hydrol.* **2015**, *524*, 696–700. [[CrossRef](#)]
13. Merabti, A.; Meddi, M.; Martins, D.S.; Pereira, L.S. Comparing SPI and RDI Applied at Local Scale as Influenced by Climate. *Water Resour. Manag.* **2018**, *32*, 1071–1085. [[CrossRef](#)]
14. Abadi, M.; Gordon, A.D. A calculus for cryptographic protocols: The spi calculus. In Proceedings of the 4th ACM Conference on Computer and Communications Security, Zurich, Switzerland, 1–4 April 1997; Volume 148, pp. 1–70.
15. Thornthwaite, C.W. An Approach Toward a Rational Classification of Climate. *Soil Sci.* **1948**, *38*, 55–94.
16. Yamamoto, R.; Iwashima, T.; Kazadi, S.N.; Hoshiai, M. Climatic Jump—A Hypothesis in Climate Diagnosis. *J. Meteorol. Soc. Jpn.* **1985**, *63*, 1157–1160. [[CrossRef](#)]
17. Fu, C.; Wang, Q. The Definition and Detection of the Abrupt Climatic Change. *Chin. J. Atmos. Sci.* **1992**, *16*, 482–493.
18. Xue, Y.; Han, P.; Feng, G. Change Trend of the precipitation and Air Temperature in Xinjiang since Recent 50 Years. *Arid Zone Res.* **2003**, *20*, 127–130.
19. Yi, X.S.; Li, G.S.; Yin, Y.Y. Spatio-temporal variation of precipitation in the Three-River Headwater Region from 1961 to 2010. *J. Geogr. Sci.* **2013**, *23*, 447–464. [[CrossRef](#)]
20. Xu, K.; Yang, D.W.; Yang, H.B.; Li, Z.; Qin, Y.; Shen, Y. Spatio-temporal variation of drought in China during 1961–2012: A climatic perspective. *J. Hydrol.* **2015**, *526*, 253–264. [[CrossRef](#)]